THE JOURNAL OF BIOLOGICAL CHEMISTRY
Vol. 279, No. 7, Issue of February 13, pp. 5708–5715, 2004

Printed in U.S.A.

The c-Jun Dimerization Protein 2 Inhibits Cell Transformation and Acts as a Tumor Suppressor Gene*

Received for publication, July 15, 2003, and in revised form, November 18, 2003
Published, JBC Papers in Press, November 19, 2003, DOI 10.1074/jbc.M307608200

Ronit Heinrich‡, Erella Livne§, Offer Ben-Izhak¶, and Ami Aronheim‡‖

From the Departments of ‡Molecular Genetics and §Anatomy, The B. Rappaport Institute in the Medical Sciences, Faculty of Medicine and the ¶Department of Pathology, Ramabam Medical Center and Faculty of Medicine, Technion-Israel Institute of Technology, Haifa Israel 31096

The c-Jun dimerization protein, JDP2, is a member of the AP-1 (activating protein-1) family of the basic leucine zipper transcription factors. JDP2 can bind 12-*O*-tetradecanoylphorbol-13-acetate (TPA)-responsive element and cAMP-responsive element DNA response elements, resulting in the inhibition of transcription. Although the role of AP-1 in cell proliferation and malignant transformation is well established, the role of JDP2 in this process is of subject to debate. On the one hand, JDP2 was shown to inhibit cyclin D transcription and promote differentiation of skeletal muscle and osteoclast cells. On the other hand, JDP2 was shown to partially transform chicken embryo fibroblast and was identified in a screen for oncogenes able to collaborate with the loss of $p27_{kip}$ cyclin-dependent inhibitor to induce lymphomas. Using cell transformation assays in NIH3T3 cells and injection of prostate cancer cell lines overexpressing JDP2 into severe combined immuno-deficient (SCID) mice, we show for the first time the potential role of JDP2 in inhibition of cell transformation and tumor suppression. The mechanism of tumor suppressor action of JDP2 can be partially explained by the generation of inhibitory AP-1 complexes via the increase of JunB, JunD, and Fra2 expression and decrease of c-Jun expression.

The activating protein-1 (AP-1)[1] plays a major role in development, proliferation, and apoptosis. AP-1 is composed of a dimeric combinatorial complex of members of the Jun homodimers (c-Jun, JunD, and JunB) or Jun heterodimer with Fos family members (c-Fos, Fos B, Fra1, and Fra2) (reviewed in Refs. 1 and 2). The Jun dimerization protein, JDP2, was identified following a two-hybrid screen with c-Jun leucine zipper as bait (3). JDP2 is a *bona fide* member of the basic leucine zipper family. Thus, similar to the Jun family members, JDP2, is able to bind DNA as a homo- and a heterodimer (3, 4). Following dimerization with Jun members, DNA binding is potentiated, but transcription of AP-1-dependent genes is inhibited. JDP2 inhibits transcription by multiple mechanisms that involve competition on DNA binding and generation of inactive AP-1 complexes and act through the indirect recruitment of histone deacetylase 3 (5). JDP2 is expressed in all cell lines tested, and similar to the other members of the AP-1 family, it is regulated at multiple levels. JDP2 is rapidly phosphorylated on threonine 148 by JNK and p38 in response to stress stimuli (6, 7). The precise role of JDP2 phosphorylation for its biological function is currently unknown. A number of processes such as skeletal muscle cell differentiation (8) and osteoclast differentiation (9) were shown to increase JDP2 protein expression levels. JDP2 was found to interact with CCAAT/enhancer-binding protein-γ, a member of the CAAT family (10), ATF2 (4), and the progesterone receptor, a member of the steroid hormone family (11). JDP2 serves as a co-activator of transcription for the progesterone receptor via direct interaction with pCAF and p300/CBP co-activators (11). Although JDP2 efficiently counteracts AP-1 action (3), it was identified as a candidate oncogene in a high throughput viral insertional mutagenesis screen collaborating with $p27_{kip}$ loss of function mutation (12). Consistent with this result, JDP2 was found to transform chicken embryo fibroblast but failed to induce anchorage-independent growth in these cells (13). Here we show that JDP2 overexpression in NIH3T3 cells inhibits cell transformation by Ras. We also tested the expression levels of JDP2 in a number of human tumors and found that only a minor fraction of tumors express higher levels of JDP2 as compared with normal cells. In addition, we used a hormone-independent prostate carcinoma cell line as a model for tumorogenesis in SCID mice to show that JDP2 strongly inhibits tumor cell growth. JDP2 action as a tumor suppressor gene inhibits AP-1 activity through the increase of JunB, JunD, and Fra2 protein levels and decrease of c-Jun expression. This is the first demonstration of JDP2 to act as a tumor suppressor gene both *in vitro* and *in vivo*.

EXPERIMENTAL PROCEDURES

Cell Culture—LNCaP, PC-3, and DU-145 prostate carcinoma cell lines were maintained in RPMI 1640 without phenol red, supplemented with 10% fetal calf serum, gentamycin (50 μg/ml), HEPES buffer 0.1 M (pH 7.3), insulin (2 μg/ml), glutamine (0.292 mg/ml), and transferrin (15 μg/ml). NIH3T3 cells were maintained in Dulbecco's Eagle's medium supplemented with 10% fetal calf serum, penicillin, and streptomycin.

Foci Formation Assay—NIH3T3 cells were transfected as described in Ref. 14. In principle, a total of 1.1 μg of pCEFL expression plasmid was transfected with 10 μg of carrier DNA using calcium phosphate precipitation method. PCEFL-RasV12 (100 ng) was used for co-transfection together with 1 μg of either pCEFL vector or pECFL-HA-JDP2 expression plasmids. DNA precipitate was left on cells overnight and washed three times with PBS the next day. Cells were grown in 5% calf

* This work was partially supported by a Research Career Development Award from the Israel Cancer Research Foundation, by the International Union Against Cancer (UICC) American Cancer Society International Fellowships for beginning investigators and CapCure Israel (to A. A.). The costs of publication of this article were defrayed in part by the payment of page charges. This article must therefore be hereby marked "*advertisement*" in accordance with 18 U.S.C. Section 1734 solely to indicate this fact.

‖ To whom correspondence should be addressed: Dept. of Molecular Genetics, The B. Rappaport Faculty of Medicine, 7 Efron St., Bat-Galim, Haifa Israel 31096. Tel.: 972-4-8295226; Fax: 972-4-8295225; E-mail: Aronheim@tx.technion.ac.il.

[1] The abbreviations used are: AP-1, activating protein-1; JDP, c-Jun dimerization protein; JNK, c-Jun NH_2-terminal kinase; BrdUrd, 5′-bromo-2′-deoxy-uridine; TPA, 12-*O*-tetradecanoylphorbol-13-acetate; TRE, TPA-responsive element; TUNEL, terminal deoxynucleotidyltransferase-mediated dUTP nick end-labeling; SCID, severe combined immuno-deficient.

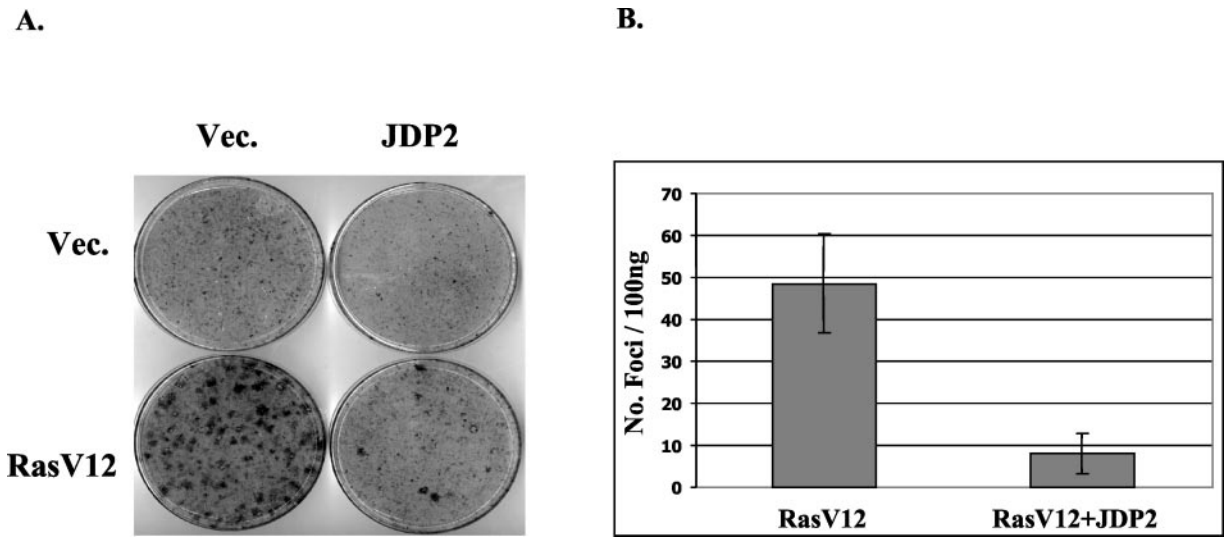

FIG. 1. **JDP2 inhibits foci formation by Ras in tissue culture.** NIH3T3 cells were transfected with the indicated plasmids. PCEFL-RasV12 (100 ng) was used in co-transfection with either pCEFL-HA-JDP2 or pCEFL expression plasmids (1 μg). Cells were cultured for 14 days in 5% calf serum and subsequently fixed and stained with crystal violet (*A*). The mean and standard deviation of foci number obtained with RasV12 cotransfections with either pCEFL (*Vec*, vector) or pCEFL-HA-JDP2 from four independent experiments is shown (*B*).

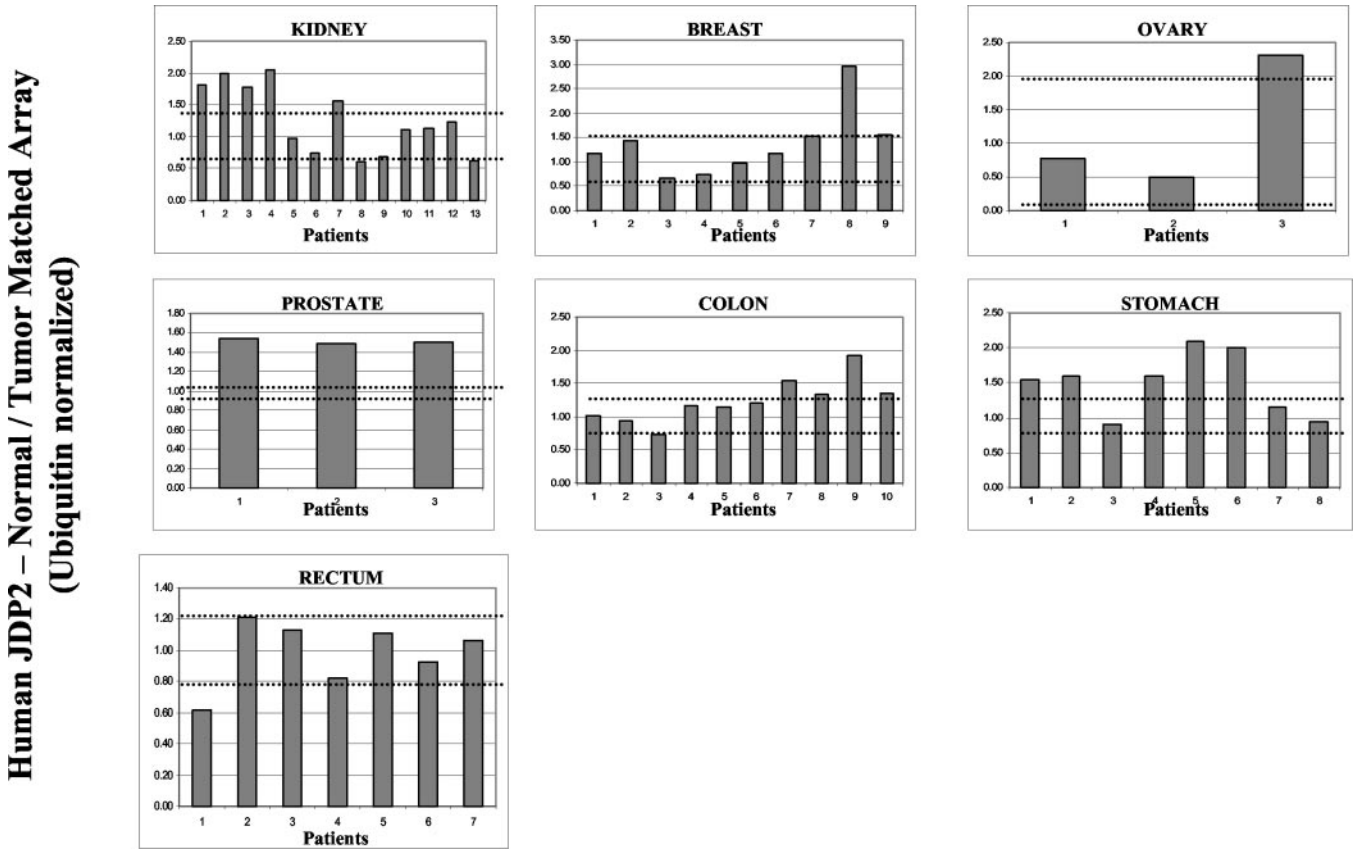

FIG. 2. **JDP2 expression levels in human panel tumors.** JDP2 mRNA expression was measured on a human tumor/normal expression array membrane (Clontech). Densitometric values were normalized to those for ubiquitin. The ratio obtained between normal and tumor tissue of each patient is shown. The *broken line* represent the standard deviation obtained from the JDP2/ubiquitin ratio derived from the normal tissues.

serum, and medium was replaced every 3 days. Following 14 days, cells were fixed in 10% methanol and 10% acetic acid for 5 min and stained with 1% crystal violet.

Matched Tumor/Normal Expression Array—The array membrane includes SMART™-amplified cDNA from 68 tumor and corresponding normal tissues from individual patients (Clontech catalog number 7840-1). In total, seven different tumors represented by at least three patients (total of 53 patients) were analyzed. JDP2 was detected by hybridization with a human JDP cDNA probe (XbaI/HindIII cut from pEBS plasmid (~500 bp) generously provided by Dr. T. Kallunki) labeled by a random priming labeling kit (Biological Industries, Beit Haemek, Israel) according to the manufacturer's instructions. Densitometric values were obtained by phosphorimaging and normalized to those found with labeled ubiquitin.

Generation of Stable JDP2-expressing Cells—PC-3 cells (passage 10) were infected with replication-defective retroviruses to generate PC-3 cell lines overexpressing JDP2. The full-length JDP2 cDNA was inserted into the pCLBabe retroviral expression plasmid by EcoRI digestion. Retroviruses expressing JDP2 or empty vector (as control) were generated by transfection into a viral packaging cell line 293gp, ex-

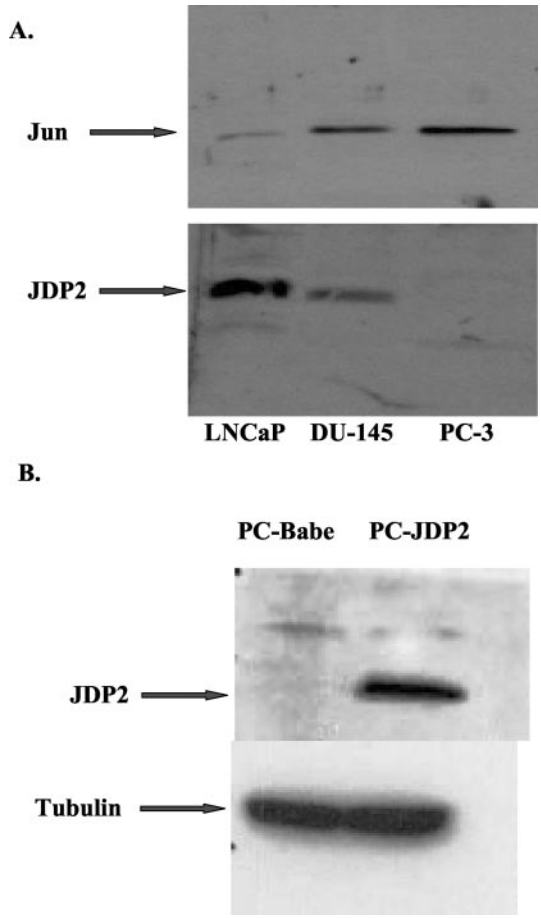

FIG. 3. **JDP2 expression in prostate cancer cell lines.** As shown in *A*, nuclear extracts (20 μg/lane), derived from LNCaP, PC-3, and DU-145 prostate carcinoma cell lines, were separated by 12.5% SDS-PAGE and immobilized to Hybond nitrocellulose membrane (Amersham Biosciences). Western blot analysis was performed with either anti-c-Jun antibody (Santa Cruz Biotechnology) or anti-JDP2 antibody. As shown in *B*, whole cell extracts (100 μg/lane) derived from either PC-JDP2 or PC-Babe stable cell lines were separated and immobilized to nitrocellulose membrane as described under "Experimental Procedures." Western blot analysis was performed using either anti-JDP2 or anti-tubulin primary antibodies. Horseradish peroxidase-conjugated goat anti-rabbit or goat anti-mouse, respectively, were used as secondary antibodies followed by chemiluminescent reaction and autoradiography.

pressing the *gag* and *pol* genes (15). The medium of transfected 293gp cells containing retroviruses was used to infect PC-3 cells. Infected cells were selected with puromycin (3 μg/ml) and pooled following 2 weeks of selection.

Tumor Generation in Mice—SCID mice (7–8 weeks old) were injected subcutaneously with the different PC-3 stable cell lines (10^7 cells/mouse). Three weeks later, when tumors developed, mice were administered intraperitoneally with 5′-bromo-2′-deoxy-uridine (BrdUrd, catalog no. 280879, Roche Applied Science; 2 mg/10 g of body weight) 2 h before euthanization. Tumors were dissected, weighted, and fixed in 4% neutral buffered formaldehyde solution (containing 4% formaldehyde, 0.4% sodium phosphate monobasic, and 0.65% sodium phosphate dibasic anhydrous).

Fluorescence-activated Cell Sorter Analysis—PC3 cell lines (0.5×10^6) were serum-starved for 72 h and then were stimulated with 5% serum for 24 h. Cells were washed once in PBS and resuspended in 1 ml of PBS at room temperature. Ice-cold absolute ethanol was added (4 ml) for cell fixation with high speed vortexing. Cells were left in ethanol at −20 °C for 15 min. Ethanol was discarded, and cells were rehydrated in PBS and incubated in the presence of 50 μg/ml RNase at 37 °C for 0.5 h. Cells were collected by centrifugation and resuspended in 1 ml of staining buffer (100 mM Tris, pH 7.4, 150 mM NaCl, 1 mM $CaCl_2$, 0.5 mM $MgCl_2$, 0.1% Nonidet P-40), and propidium iodide (Molecular Probes Inc., 1 μg/ml) was added to cell suspension for 15 min at room temperature followed by flow cytometry analysis.

TUNEL Staining—Sections were stained by the *in situ* death detection POD kit (Roche Diagnostics), according to the manufacturer's instructions, modified as described (16).

Western Blot Analysis—Whole cell extracts and nuclear extracts were prepared and collected as described previously (17, 18). For protein extraction from tumor slices, ~1 g of tissue was homogenized in ~3 ml of ice-cold radioimmune precipitation assay buffer (containing 1% Nonidet P-40, 0.5% sodium deoxycholate, and 0.1% SDS in PBS supplemented with protease inhibitor mixture) followed by a 30-min incubation. Total cell lysates were collected after centrifugation at 10,000 × *g* for 10 min at 4 °C. Proteins were separated on a 12.5% SDS-PAGE and electroblotted on a Hybond membrane (Amersham Biosciences). Membranes were incubated in 5% nonfat dry milk in PBS for 1 h and subsequently probed with the following primary polyclonal antibodies: anti-c-Jun, anti-JunD, anti-JunB, and anti-Fra2 (all purchased from Santa Cruz Biotechnology) and anti-JDP2 (3). Anti-tubulin monoclonal antibody (Sigma) was used for protein loading control levels. Horseradish peroxidase-conjugated goat-anti-rabbit or goat-anti-mouse (Jackson ImmunoResearch Laboratories, Inc.) were used as secondary antibodies. Bound antibodies were detected using enhanced chemiluminescence reagent (Biological Industries) according to the manufacturer's instructions and visualized by autoradiography.

Histology and Immunohistochemical Stainings—Tumor slices derived from injected SCID mice were fixed in 4% neutral buffered formaldehyde, embedded in paraffin, serially sectioned at 6-μm intervals, and mounted on slides (polylysine-coated Super Frost Plus, Menzel-Glaser). Sections were routinely processed for deparaffinization through three washes of xylene followed by graded washings of alcohols (100 and 95%) for 5 min each. Tissue sections were stained with Hematoxylin and Eosin for general morphology. For hydration, slides were washed (with 5-min intervals) twice with H_2O and once with PBS. For antigen unmasking, sections were heated in 10 mM sodium citrate buffer (pH 6.0) for 10 min, and then washed three times (with 5-min intervals) with H_2O and once with PBS. Nonspecific binding was blocked with 5% fetal calf serum in PBS for 1 h at room temperature followed by the addition of anti-BrdUrd monoclonal antibody (DAKO ALS, Glostrup, Denmark) diluted 1:25 in blocking solution overnight at 4 °C. Sections were washed with PBS followed by the addition of Rhodamine Red-X-conjugated donkey anti-mouse IgG (Jackson ImmunoResearch Laboratories, Inc.), diluted 1:100 in blocking solution, for 1 h at room temperature. Following three PBS washings, nuclei were stained for 10 min at room temperature with 4′,6-diamidino-2-phenylindole (Sigma, prepared as 1 mg/ml H_2O stock and diluted 1:1000 in PBS) followed by washings in PBS. The tumor sections were stained with primary anti-active caspase-3 (R&D Systems Inc.) diluted 1:3000 followed by washing and detected by the streptavidin-biotin complex method as described previously (16). Sections were visualized using an Olympus Model BX50 fluorescence microscope at a magnification of ×200 and were photographed with a digital camera.

RESULTS

Inhibition of Ras Transformation in NIH3T3 Cells—The overexpression of JDP2 in chicken embryo fibroblast resulted in the loss of contact inhibitory cell growth and generation of foci characteristic of cell transformation (13). To test the ability of JDP2 to transform mammalian cells, NIH3T3 cells were transfected with either pCEFL expression vehicle plasmid or pCEFL expression plasmid encoding for HA-JDP2. Cells were grown to high density for 2 weeks in 5% calf serum. The cells transfected with JDP2 exhibited contact-inhibited growth similar to the vector control-transfected cells (Fig. 1*A*). This result prompted us to examine the ability of JDP2 to inhibit cell transformation by a well established oncogene. Toward this end, we co-transfected NIH3T3 cells with pCEFL-RasV12 expression plasmid together with either vector control or expression plasmid encoding for JDP2. Although Ras-transfected cells exhibited loss of contact growth inhibition and typical foci formation, cells co-transfected with RasV12 together with JDP2 exhibited a significant reduction in size, and only 16% of the number of foci formed as compared with RasV12 alone (Fig. 1, *A* and *B*), suggesting that JDP2 has a potential to serve as a tumor suppressor gene.

JDP2 Expression in Human Tumors—To examine whether differential JDP2 gene expression may be relevant to human

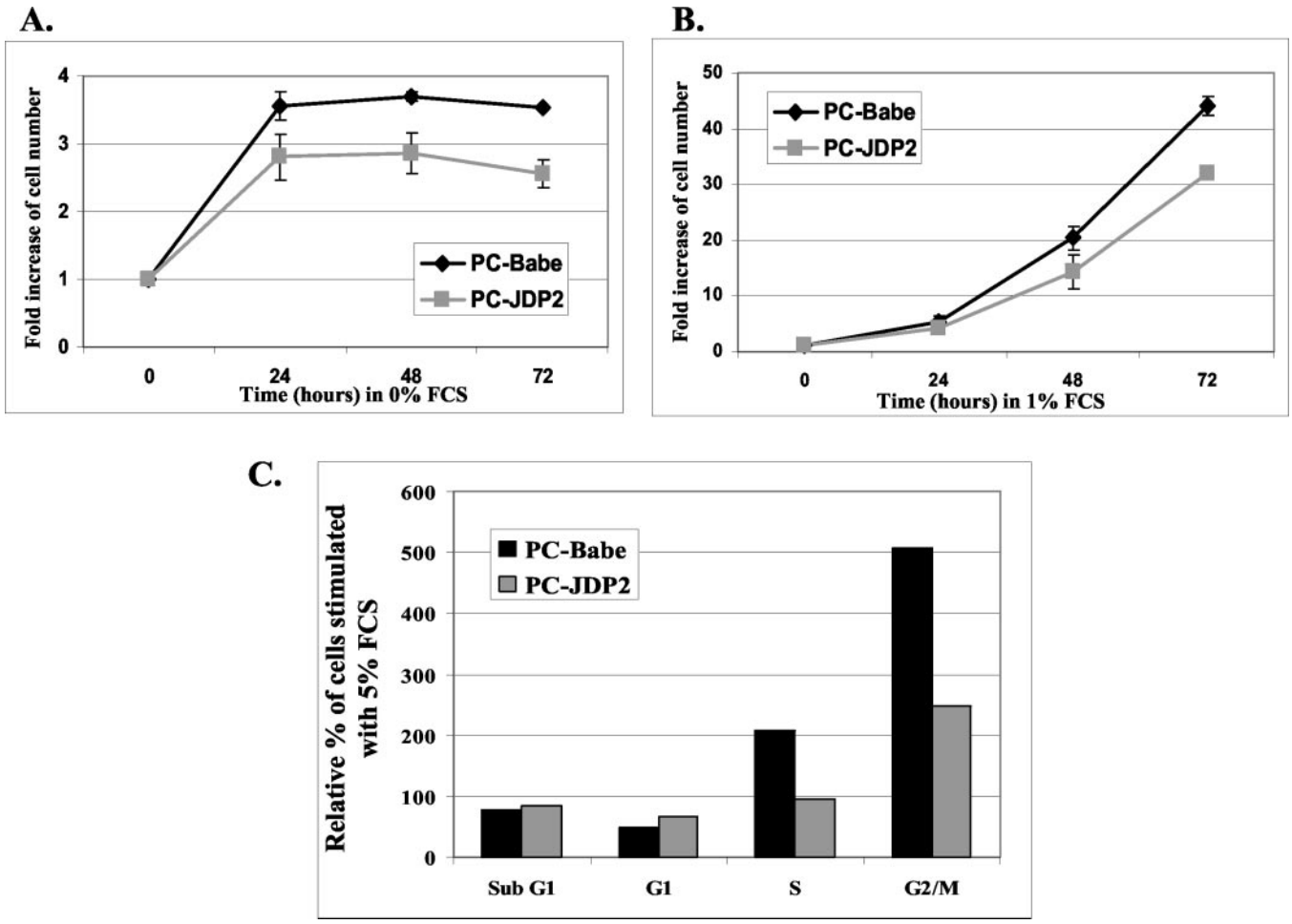

FIG. 4. **JDP2-dependent inhibition of proliferation *in vitro*.** PC-JDP2 and PC-Babe control stable cell lines were seeded, at 0.5×10^6 cells, in 10-cm plates in either serum-free medium (*A*) or 1% serum (*B*) for the indicated time points. The number of live cells was determined as the mean ± S.E. of three independent experiments. *FCS*, fetal calf serum. As shown in *C*, serum-starved cells (72 h) were stimulated with 5% serum for 24 h, and the cell cycle was tested by fluorescence-activated cell sorter analysis. The results are presented as the percentage of cells found in 5% serum *versus* serum-starved cells in each phase of the cell cycle. For each cell cycle phase analyzed, 100% was determined as the number of cells found in serum-starved condition. The results represent the mean of two independent experiments.

cancer, we have used a matched tumor/normal expression array nylon membrane (Clontech) in which cDNA samples derived from 53 patients diagnosed with cancer were immobilized to membrane representing seven different tumors. From each patient, a pair of cDNA samples was derived from the tumor and the corresponding normal tissue as a control. We probed the membrane with radiolabeled hJDP2 cDNA and determined the level of radioactivity obtained in the normal tissue as compared with the level obtained in the tumor. A housekeeping gene, ubiquitin, was used to correct for cDNA loading deviations (Fig. 2). Although 58.4% of patients exhibited no change in JDP2 expression levels, 35.8% of patients exhibited higher levels of expression of JDP2 in normal tissue as compared with the matched tumor tissue. Only a small percentage (5.7%) of patient-derived tumors exhibited significantly higher JDP2 levels in the tumor as compared with the normal tissue. From this analysis, we concluded that JDP2 is more likely to play a role as a tumor suppressor gene. However, one cannot exclude the possibility that in specific genetic lesions, overexpression of JDP2 may be involved in or play a role in tumorogenesis of human cancer.

JDP2 Expression in Prostate Cancer Cell Lines—Since prostate cancer patients (3 out of 3 patients) exhibited elevated JDP2 levels in normal tissue as compared with the tumor tissues (Fig. 2), we decided to focus our further analysis on prostate cancer cell lines. First, we examined the level of JDP2 and c-Jun protein in Western blots with nuclear extract derived from three different prostate carcinoma cell lines using the corresponding antibodies. Nuclear extract was prepared from LNCaP, representing the androgen-dependent cell line, and two androgen-independent aggressive prostate cancer cell lines, DU-145 and PC-3. Although JDP2 protein levels were found relatively high in LNCaP cells, the expression was much lower in DU-145 and undetectable in PC-3 cell-derived extracts (Fig. 3*A*, *lower panel*). Moreover, c-Jun showed reverse correlation with JDP2 expression in these cell lines, *i.e.* c-Jun was barely detectable in LNCaP cells and in relatively high levels in both DU-145 and PC-3 cell-derived extracts (Fig. 3*A*, *upper panel*).

Ectopic Expression of JDP2 in a PC-3-derived Cell Line—The androgen-independent prostate cell line, PC-3, exhibited the lowest level of JDP2 expression. Therefore, we next studied the consequence of ectopic expression of JDP2 in these cells. We used either the pBabe retrovirus expression vector control or the pBabe-JDP2 expression vector to infect the 293gp-packging-cell line to produce the corresponding retroviruses. Retroviruses produced were used to infect PC-3 cells that were subsequently selected for puromycin resistance. The cell lines generated were designated PC-Babe and PC-JDP2, respectively. Nuclear extract derived from these cell lines was subjected to Western blot analysis with JDP2-antibodies and tubulin-antibodies. The latter served as loading control. A strong

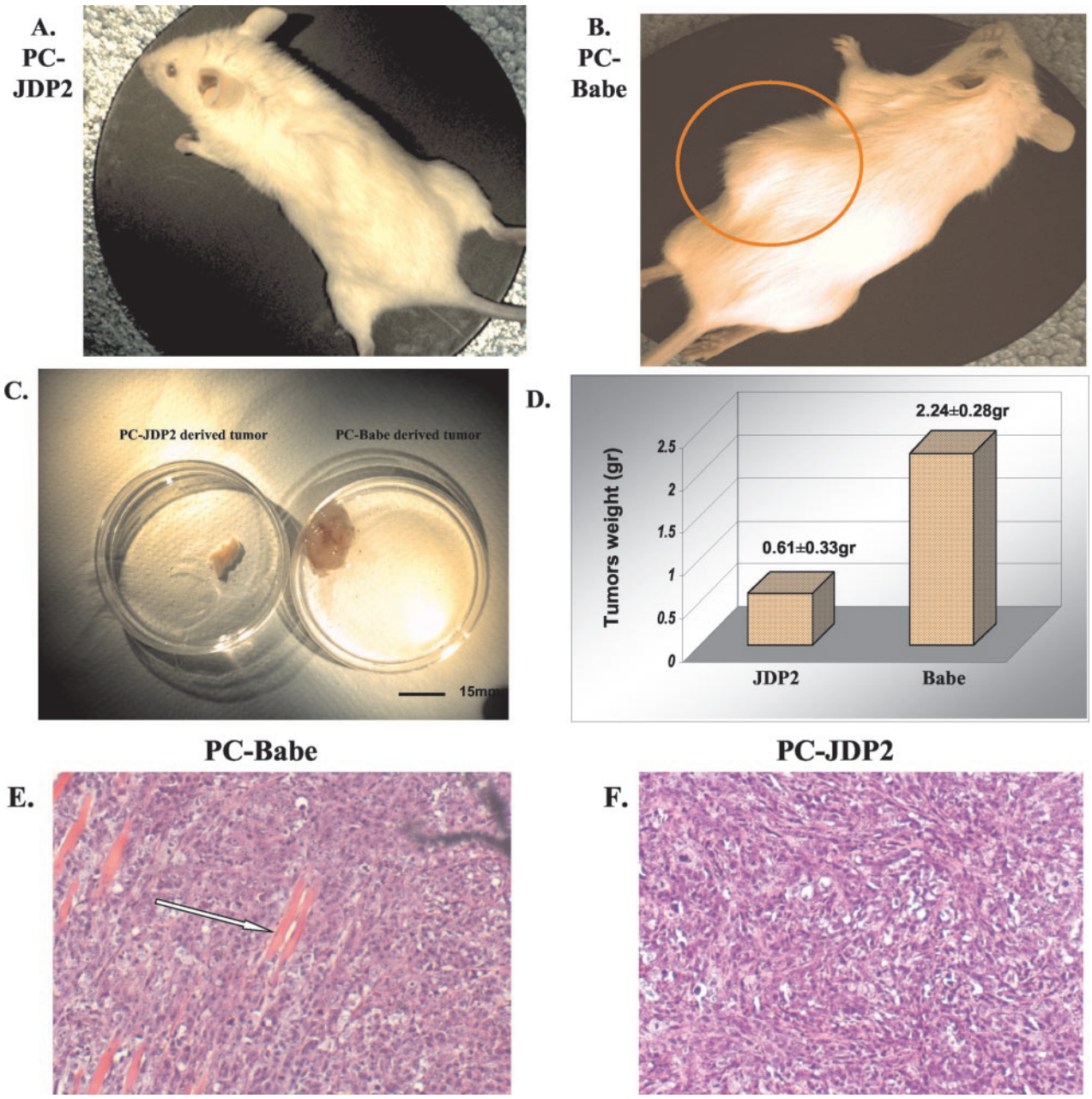

FIG. 5. **PC-3 stable cell line-derived tumors.** Cells derived from PC-JDP2 and PC-Babe stable cell lines were injected (10^7 cells/mouse) subcutaneously to 7-month-old SCID mice. Three weeks later, when tumors developed (*A* and *B*), mice were sacrificed, and tumors were dissected out (*C*) and weighted (*D*). Representative mice and tumors are shown. The results presented are derived from at least 12 mice in each group and represent the mean ± S.D. Hematoxylin and eosin staining of PC-Babe- and PC-JDP2-derived tumors is shown (*E* and *F*, respectively). Congested blood capillaries (*arrow*) are indicated in the control PC-Babe tissue (*E*).

cross-reacting band corresponding to the 18-kDa JDP2 protein was observed in the PC-JDP2-derived extract. The endogenous JDP2 expression level, however, was below the detection sensitivity in the PC-Babe control cell line (Fig. 3*B*, *upper panel*). The expression of tubulin was similar in both cell lines (Fig. 3*B*, *bottom panel*), suggesting that the high expression of JDP2 in PC-JDP2 cells is the result of stable integration of the virus into the cell genome.

The PC-JDP2 cell line exhibited slower growth rate as compared with the PC-Babe control cell line. Culturing cells in the absence (Fig. 4*A*) or in the presence of 1% serum (Fig. 4*B*) showed that PC-JDP2 cells have slower growth rate and lower saturation density as compared with PC-Babe control cells. Serum-starved PC-Babe cells stimulated by 5% serum for 24 h exhibited 2- and 5-fold increase in cells entering to S and G_2/M phases, respectively, whereas PC-JDP2 cells exhibited only 2.3-fold increase in the number of cells found in G_2/M phase. No significant changes were observed in the number of PC-JDP2 cells entering to S phase (Fig. 4*C*). Moreover, PC-Babe and PC-JDP2 cell lines showed no significant difference in the number of cells found in apoptotic sub-G_1 phase. Taken together, these results suggest that JDP2 overexpression resulted in an inhibition of cell growth *in vitro*.

JDP2 Inhibits Cell Growth of PC-3 Cells in SCID Mice—To examine whether the slower growth rate of cells ectopically expressing JDP2 also reduced their tumorogenic potential, we injected 10^7 cells subcutaneously into SCID mice and followed tumor growth 3 weeks after injection. In control mice injected with PC-Babe cells, large tumors were readily observed, whereas in mice injected with PC-JDP2 cells, significantly smaller tumors as compared with PC-Babe-injected mice were observed (Fig. 5, *A* and *B*). Tumors were dissected from a total

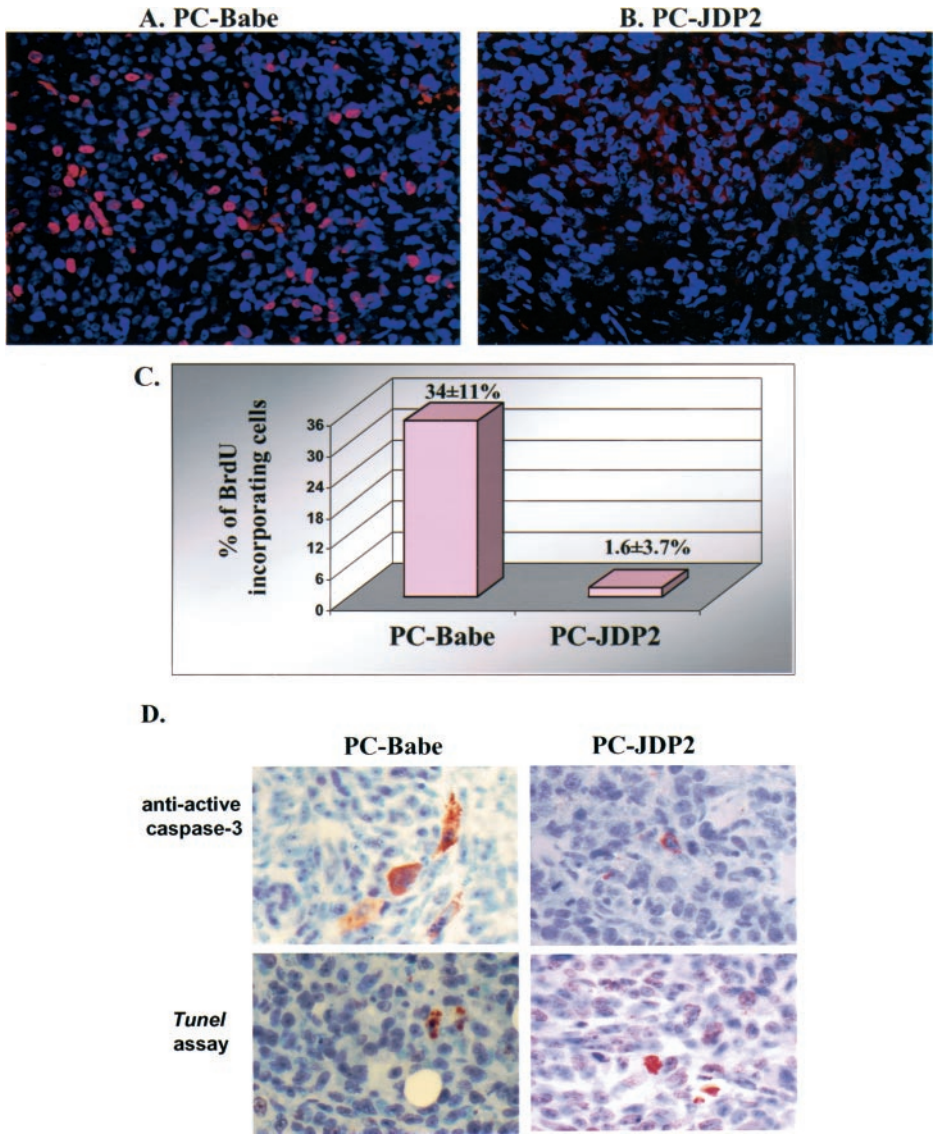

FIG. 6. **JDP2-dependent suppression of DNA synthesis in PC-3-derived tumors.** Mice described in the legend for Fig. 5 were administered intraperitoneally with BrdUrd (2 mg/10 g of body weight) 2 h prior to tumor dissection and fixation in 4% neutral buffered formaldehyde. Paraffin-embedded tissues from mice injected with PC-Babe (*A*) and PC-JDP2 (*B*) were immunostained with anti-BrdUrd antibodies (*red staining*). Cell nuclei were visualized by 4′,6-diamidino-2-phenylindole (*blue staining*). Representative co-stained fields are shown. As shown in *C*, BrdUrd-labeled cells were counted relative to the number of nuclei. The results presented were derived from tumors excised from 12 mice in which at least 20 fields consisting of 200 cells each and represent the mean ± S.D. *BrdU*, BrdUrd. *D*, immunohistochemical staining for anti-active caspase-3 (*upper panels*) and TUNEL assay (*bottom panels*) with paraffin-embedded sections of PC-Babe (*left panels*) and PC-JDP2 (*right panels*)-derived tumors.

of 12 mice, and the weight of each tumor was determined (Fig. 5, *C* and *D*). The tumors derived from PC-JDP2-injected mice were significantly smaller in size (3.7-fold) as compared with tumors derived from PC-Babe-injected mice. In addition, the histology of the tumor derived from PC-Babe-injected mice showed densely packed cells and congested capillaries, whereas in the PC-JDP2-injected tumors, the cells were more dispersed within the tissue, and the capillaries appeared normal (Fig. 5, *E* and *F*). Both PC-Babe- and PC-JDP2-derived tumors were defined as solid, anaplastic, infiltrative, with a high Gleason-grade of 10 (5 + 5)/10 (19). To determine the proliferation rate of the tumors, mice were administered with BrdUrd at 2 h prior to euthanization. Tumors were fixed, and paraffin-embedded tissues were stained with anti-BrdUrd antibodies (Fig. 6, *A* and *B*). Although 34% of cells derived from PC-Babe-injected tumors were positive for BrdUrd incorporation, only about 2% of cells derived from PC-JDP2-injected tumors showed proliferation capacity (Fig. 6*C*). Since smaller tumor size can result from increase in cell death as well, we examined apoptosis in PC-Babe- and PC-JDP2-derived tumor sections for activated caspase-3 and by TUNEL assay (Fig. 6*D*). In both assays, no significant changes were observed between PC-Babe- and PC-JDP2-stained sections, suggesting that cell proliferation is more likely to explain the differences in tumor size.

Increased Expression of JunB, JunD, and Fra2—To verify that JDP2 expression is maintained in the tumors excised from the mice, tumor-derived tissues were lysed in radioimmune precipitation assay buffer buffer followed by homogenization. Total cell lysate of the tumors was subjected to SDS-PAGE followed by Western blotting with anti-JDP2 antibodies (Fig. 7*A*). Consistent with the expression of JDP2 in the PC-JDP2 cell line, JDP2 was highly expressed in the tumor. In addition, we measured the level of expression of several AP-1 family members using Western blot analysis. We observed increased levels of JunB, JunD, and Fra2 (Fig. 7*A*), whereas c-Jun levels were dramatically decreased. Consistent with this, we observed an increase in total human collagenase-TRE DNA binding activity in lysate derived from PC-JDP2-derived tumor (Fig. 7*B*). This result suggests that ectopic expression of JDP2 resulted in the generation of a well established anti-proliferative AP-1 complex.

DISCUSSION

JDP2 was shown to repress transcription from TRE and cAMP-responsive element DNA elements and to inhibit AP-1-dependent transcription activity (3). Although the role of AP-1 in cell proliferation and cancer is well established (2), the role of JDP2 in malignant cell transformation is currently under

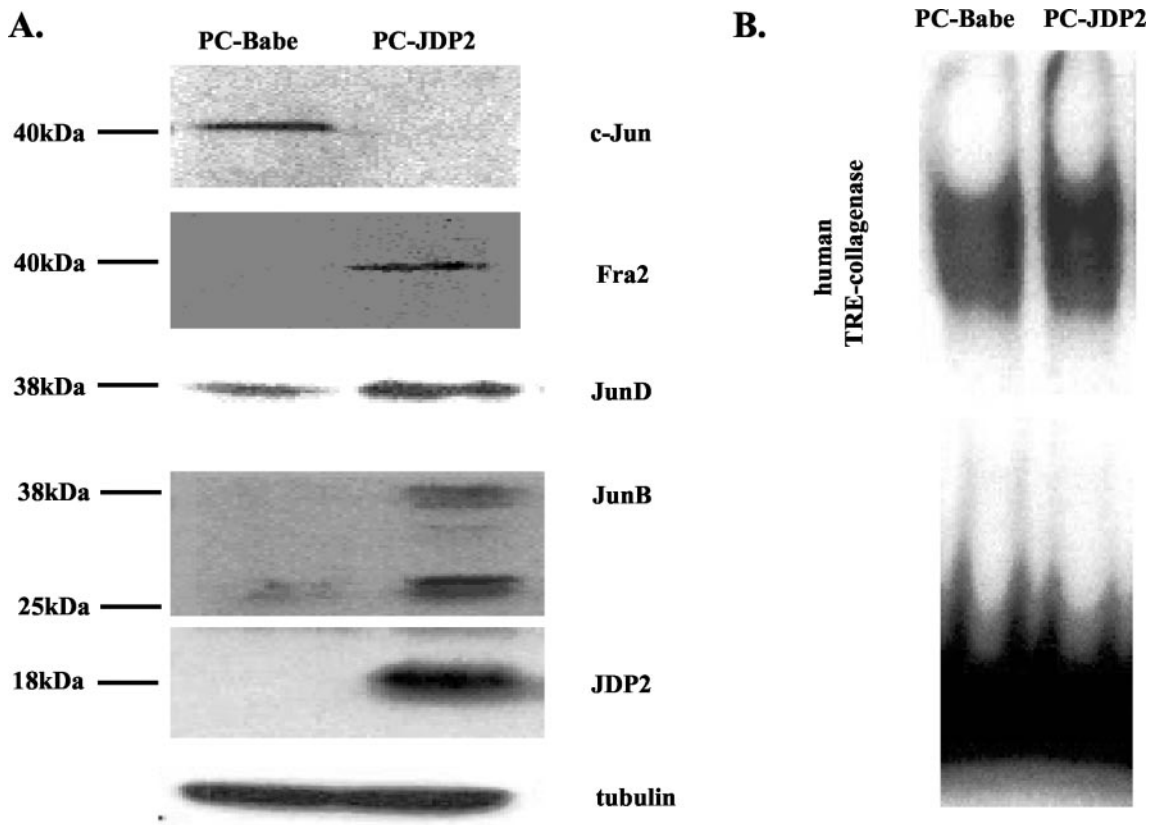

FIG. 7. **AP-1 expression in tumors.** *A*, Western blot analysis of cell lysate derived from the indicated tumors as described in the legend for Fig. 3. Membranes were probed with anti-tubulin, anti-JDP2, anti-JunB, anti-JunD, anti-c-Jun, and anti-Fra2 antibodies. Horseradish peroxidase-conjugated goat anti-rabbit was used as secondary antibody followed by chemiluminescent reaction and autoradiography. As shown in *B*, cell lysate (15 μg) was used in electrophoretic mobility shift assay using human collagenase labeled TRE DNA probe. Electrophoresis was performed in 0.5× TBE at 4 °C. Gels were fixed, dried, and exposed to autoradiography.

debate. In the above study, we provide strong evidence for the role of JDP2 in inhibition of tumorigenesis. First, JDP2 efficiently inhibited Ras-dependent cell transformation in NIH3T3 cells. Second, we showed that in a human tumor panel consisting of 53 patients, only a small fraction (5.7%) of cancer patients display higher expression of JDP2 in the tumors as compared with the normal tissues. In the latter case, it is unlikely that the high levels of JDP2 are responsible for the initiation of tumorogenesis but are probably the result of the tumor progression or are important for tumor maintenance. Understanding the mechanism for JDP2 overexpression in those tumors is of great importance since JDP2 may have tumor suppressor function in other tumors, and therefore, manipulating JDP2 expression levels may be used to inhibit malignant transformation.

Third, interestingly, we observed a high incidence of loss of JDP2 expression in prostate cancer patients (representing prostate adenocarcinoma) and in cell lines (PC-3 and DU-145) representing more aggressive and progressive stages of the disease. Importantly, ectopic expression of JDP2 in PC-3 significantly reduced its proliferative properties both *in vitro* and *in vivo*. In addition, no significant differences were observed when apoptotic markers were examined, therefore suggesting that cell proliferation but not cell death is more likely to be an explanation for the differences found in tumor size.

The present study showed that tumors derived from PC-Babe-injected mice developed large, highly vascularized tissue. These tumors are characterized with a higher proliferating index as compared with the PC-JDP2-derived tumors, which may explain the differences observed in the tumor vascularization and thus are not necessarily a direct consequence of JDP2 expression.

JDP2 was shown previously to serve as a co-activator of the progesterone receptor (11). Since the lack of detectable JDP2 protein correlates with loss of androgen-dependence, it may be possible that JDP2 cooperates with the androgen receptor in the initial stages of androgen-dependent prostate cancer, and either upon loss or upon part of the transition to androgen-independent stage, JDP2 expression is lost. Thus, it would be interesting to test the possible cooperation between the androgen receptor and JDP2.

Previous work with dominant negative mutants of c-Jun, designated TAM67, also demonstrated the ability of this artificial reagent to inhibit AP-1-dependent breast cancer tumor growth (20). However, the mechanism suggested for inhibition was through the inhibition of the major AP-1 component c-Jun and inhibition of transcription of Jun-dependent genes important for cell cycle progression, such as cyclin D1, and therefore, highlighting c-Jun importance in multiple malignant cell transformation. In this study, the ectopic expression of JDP2, an otherwise ubiquitously expressed protein, was shown to inhibit cell transformation. The results, on the one hand, establish the role of JDP2 as a tumor suppressor gene, and on the other hand, may provide a potential therapeutic tool for inhibition of cell transformation upon JDP2 overexpression. In addition, the mechanism of JDP2 inhibition of cell transformation is not solely dependent on inhibition of AP-1-dependent transcription but also can be explained in part by increasing the expression levels of JunB, JunD, and Fra2. JunB was shown to increase the expression of $p16_{ink4a}$ (21), whereas JunD was shown to collaborate with the tumor suppressor protein, Menin (22), to inhibit cell growth. Interestingly, the shorter (34 kDa) JunB species found in PC-JDP2-derived tumor (Fig. 7*A*) is associated with quiescent postmitotic cell state

(23). PC3 cells are derived from bone metastatic lesions of a prostate cancer patient, in which the increased levels of JunD and Fra2 are correlated with post-proliferative osteoblasts (24). Further studies are required to uncover whether JDP2 directly regulates the JunB and JunD promoters or their higher expression represents indirect JDP2 effect. In addition, consistent with the ability of JDP2 to inhibit c-Jun expression in F9 cells (5), we observed a strong decrease in c-Jun expression in PC-JDP2-derived tumor lysate. Previous study has shown that JDP2 represses p53 expression; nevertheless, PC3 cells are hemizygous for mutated *p53* gene (25). Thus, p53 expression in the PC3 cell lines and tumor-derived extracts could not be detected.

In this study, we established the role of JDP2 in inhibition of cell transformation. Nevertheless, one cannot exclude the possibility that under certain genetic alterations, JDP2 cooperates in cell transformation. A case in point is the overexpression of JDP2 in the background of loss of function of $p27_{kip}$ (12) or yet to be discovered mutations. Indeed, we observed, although at low incidence, higher expression of JDP2 in tumor tissues as compared with normal tissues in the normal/tumor panel (Fig. 2); however, the fact that a combination of other genetic alterations might have occurred in these patients along with JDP2 overexpression should be further analyzed.

In addition, in chicken embryo fibroblast, JDP2 overexpression resulted in partial cell transformation (13). It was already shown that cell transformation in chicken embryo fibroblast does not necessarily represent the oncogenic potential of a given protein. For example, whereas ectopic expression of c-Jun was found to transform chicken embryo fibroblast, it was not sufficient for transformation of rat embryo fibroblast cells (26). Moreover, it was shown that JunB transforms chicken embryo fibroblast and promotes growth in soft agar (27). However, in mouse embryonic fibroblast, JunB overexpression results in premature senescence (21). Another possible explanation for the ability of JDP2 to partially transform chicken embryo fibroblast could be the lack of JunB in avian cells. In PC-JDP2-derived tumors, JunB was shown to be elevated and may explain in part JDP2 anti-proliferative action.

It would be of great interest to generate animal models in which JDP2 expression is genetically manipulated toward gain/loss of function. These animal models would enable us to determine at which stage of tumorogensis JDP2 expression is required to rescue malignant transformation and examine the contribution of loss of JDP2 expression in multiple carcinogenesis models *in vivo*.

Acknowledgments—We thank Drs. T. Kallunki for hJDP2 plasmid, H. Teramoto for assistance in Ras transformation assays, O. Shenkar for assistance in imaging, and P. Shenzer, S. Ben-Eliezer, I. Minkov, and A. Cohen for technical assistance.

REFERENCES

1. Wagner, E. F. (2001) *Oncogene* **20,** 2334–2335
2. Shaulian, E., and Karin, M. (2001) *Oncogene* **20,** 2390–2400
3. Aronheim, A., Zandi, E., Hennemann, H., Elledge, S., and Karin, M. (1997) *Mol. Cell. Biol.* **17,** 3094–3102
4. Jin, C., Ugai, H., Song, J., Murata, T., Nili, F., Sun, K., Horikoshi, M., and Yokoyama, K. K. (2001) *FEBS Lett.* **489,** 34–41
5. Jin, C., Li, H., Murata, T., Sun, K., Horikoshi, M., Chiu, R., and Yokoyama, K. K. (2002) *Mol. Cell. Biol.* **22,** 4815–4826
6. Katz, S., Heinrich, R., and Aronheim, A. (2001) *FEBS Lett.* **506,** 196–200
7. Katz, S., and Aronheim, A. (2002) *Biochem. J.* **368,** 939–945
8. Ostrovsky, O., Bengal, E., and Aronheim, A. (2002) *J. Biol. Chem.* **277,** 40043–40054
9. Kawaida, R., Ohtsuka, T., Okutsu, J., Takahashi, T., Kadono, Y., Oda, H., Hikita, A., Nakamura, K., Tanaka, S., and Furukawa, H. (2003) *J. Exp. Med.* **197,** 1029–1035
10. Broder, Y. C., Katz, S., and Aronheim, A. (1998) *Curr. Biol.* **8,** 1121–1124
11. Wardell, S. E., Boonyaratanakornkit, V., Adelman, J. S., Aronheim, A., and Edwards, D. P. (2002) *Mol. Cell. Biol.* **22,** 5451–5466
12. Hwang, H. C., Martins, C. P., Bronkhorst, Y., Randel, E., Berns, A., Fero, M., and Clurman, B. E. (2002) *Proc. Natl. Acad. Sci. U. S. A.* **99,** 11293–11298
13. Blazek, E., Wasmer, S., Kruse, U., Aronheim, A., Aoki, M., and Vogt, P. K. (2003) *Oncogene* **22,** 2151–2159
14. Zohar, M., Teramoto, H., Katz, B. Z., Yamada, K. M., and Gutkind, J. S. (1998) *Oncogene* **17,** 991–998
15. Naviaux, R. K., Costanzi, E., Haas, M., and Verma, I. M. (1996) *J. Virol.* **70,** 5701–5705
16. Nagler, R. M., Kerner, H., Laufer, D., Ben-Eliezer, S., Minkov, I., and Ben-Itzhak, O. (2002) *Cancer Lett.* **186,** 137–150
17. Hibi, M., Lin, A., Smeal, T., Minden, A., and Karin, M. (1993) *Genes Dev.* **7,** 2135–2148
18. Schreiber, E., Matthias, P., Muller, M. M., and Schaffner, W. (1989) *Nucleic Acids Res.* **17,** 6419
19. Gleason, D. F., and Mellinger, G. T. (1974) *J. Urol.* **111,** 58–64
20. Liu, Y., Ludes-Meyers, J., Zhang, Y., Munoz-Medellin, D., Kim, H. T., Lu, C., Ge, G., Schiff, R., Hilsenbeck, S. G., Osborne, C. K., and Brown, P. H. (2002) *Oncogene* **21,** 7680–7689
21. Passegue, E., and Wagner, E. F. (2000) *EMBO J.* **19,** 2969–2979
22. Agarwal, S. K., Guru, S. C., Heppner, C., Erdos, M. R., Collins, R. M., Park, S. Y., Saggar, S., Chandrasekharappa, S. C., Collins, F. S., Spiegel, A. M., Marx, S. J., and Burns, A. L. (1999) *Cell* **96,** 143–152
23. Sheerin, A., Thompson, K. S., and Goyns, M. H. (2002) *Cancer Lett.* **177,** 83–87
24. Yeung, F., Law, W. K., Yeh, C. H., Westendorf, J. J., Zhang, Y., Wang, R., Kao, C., and Chung, L. W. (2002) *J. Biol. Chem.* **277,** 2468–2476
25. Carroll, A. G., Voeller, H. J., Sugars, L., and Gelmann, E. P. (1993) *Prostate* **23,** 123–134
26. Su, Z., Shi, Y., and Fisher, P. B. (2000) *Oncogene* **19,** 3411–3421
27. Castellazzi, M., Spyrou, G., La Vista, N., Dangy, J. P., Piu, F., Yaniv, M., and Brun, G. (1991) *Proc. Natl. Acad. Sci. U. S. A.* **88,** 8890–8894